Fully differential ionization cross sections for proton collisions with multielectronic targets

S. Martínez,[1] S. Otranto,[1] and C. R. Garibotti[2]
[1]*CONICET and Departamento de Física, Universidad Nacional del Sur, 8000 Bahía Blanca, Argentina*
[2]*CONICET and Centro Atómico Bariloche, 8400 S. C. de Bariloche, Argentina*
(Received 2 November 2007; published 20 February 2008)

In this work we present a theoretical study of the single ionization process involved in collisions of protons on He, Li, and Be targets at 2 MeV/amu projectile impact energy. Fully differential cross sections (FDCSs) are calculated within a continuum distorted wave method. Three different potentials are used to represent the interaction between the low energy outgoing electron and the residual ion target. Two of them are based on Coulomb potentials with proper effective charges for the target, while the other relies in a Garvey-type potential. These procedures provide remarkable differences in the binary and recoil peak regions, for the Li and Be cases. On the other hand, He target calculations lead to qualitative agreement for the three FDCSs at the momentum transfers and emission energies here considered. These results manifest the complexity of the ionization process for multielectronic targets and emphasize the importance of choosing an adequate model potential to describe the emitted electron dynamics in ionizing collisions.

DOI: 10.1103/PhysRevA.77.024701 PACS number(s): 34.10.+x, 34.50.Fa

The study of the electron emission process in charged particle collisions with atoms represents one of the most interesting problems in atomic physics research. Since one or more target electrons are finally unbound, those studies allow for a detailed exploration of the continuum state of few-body systems.

During the last decade, recoil ion momentum spectroscopy (RIMS) has developed as a powerful experimental technique to carry on kinematically detailed experiments in ion-atom collisions [1]. The cold target recoil ion momentum spectroscopy (COLTRIMS) makes it possible to measure the momentum vectors of the ionized electron and the recoiling target ion directly and deduce the scattered projectile momentum from the momentum conservation [2]. In other words, within this technique it is possible to determine the fully differential cross section (FDCS), which provides the most detailed information on an ionizing collision.

Even though FDCSs restricted to the collision plane (coplanar configuration) have been measured in the $(e,2e)$ context for more than 35 years now [3], it was only a few years ago that FDCSs for single ionization of He by ion impact were finally reported [4]. Since then, FDCSs for the single ionization of He by C^{6+}, $Au^{24+,53+}$, and H^+ projectiles at different impact energies have been published for rather small momentum transfers [5].

The first theoretical coplanar FDCSs for single ionization in ion-atom collisions were reported in 1993 by Berakdar *et al.* for the hydrogen target [6]. A few years later, and also within a continuum distorted wave (CDW) model, the diverse features exhibited by the coplanar FDCS for the hydrogen target were identified and discussed [7–9]. These authors represented the FDCS in momentum space instead of using the electron angular distributions familiar to the $(e,2e)$ community. This representation allowed for an easy identification of the usual peaks and some ring-shaped structures associated to double collisions of the electron and projectile with the target. Almost simultaneously, theoretical FDCSs were obtained by means of the classical trajectory Monte Carlo (CTMC) model to explore ionization mechanisms as soft, saddle point, charge transfer to the continuum and binary encounter electron production for different projectiles colliding with He [10]. Since 2002, different groups have worked towards a good representation of the available data and studies have been carried out by means of different distorted wave methods and the CTMC model [11–16].

A new horizon has recently opened up in the field with the inclusion of a lithium magneto-optical trap (MOT) in a reaction microscope [18]. This will allow us to perform, in the near future, kinematically complete experiments involving collisions of charged particles and photons on Li targets. Such studies will surely challenge the versatility of the presently used models to deal with multielectronic targets.

In this work we study H^+ ionizing collisions on multielectronic targets like He, Li, and Be. The momentum transfer values considered as well as the impact energy of 2 MeV/amu were selected similar to those published for the He target. The Li target was already considered by Sánchez *et al.* at the minimum momentum transfer needed for the reaction to take place ($Q_\perp=0$) [8], identifying in the momentum representation the main visible structures over a wide range of electron energies.

Previous analysis by McCartney and Crothers using the continuum distorted waves with eikonal initial state (CDW-EIS) method has shown that the total cross section for Li $1s$-ionization due to proton impact at the present impact energy is about a factor 3 smaller than that arising from the $2s$ subshell [17]. For the Be target, this factor increases up to about 10 and for both targets the inner shell ionization becomes negligible as the impact energy is decreased. In principle, the COLTRIMS technique can resolve the contributions arising from the $1s$ and $2s$ subshells. The parallel component of the momentum transfer $Q_\parallel=\Delta E/v$ depends on the shell from where the electron is being ionized. Thus we assume that the forthcoming kinematically complete resolved experiments for ion impact on multielectronic targets will distinguish between these subshell contributions at the present regime of intermediate to high projectile energies. A straightforward estimation for the Li target at the present

impact energy of 2 MeV/amu leads to $Q_{\parallel 1s}=0.06$ a.u. and $Q_{\parallel 2s}=0.28$ a.u. which are about a factor 4.6 from each other. In the following, we restrict ourselves to the valence shell and analyze the main trends associated to the FDCS when the emission is originated from the $n=2$ level.

To obtain the FDCS, we evaluate the ionization transition matrix T_{fi} by means of a CDW model similar to that used in Refs. [11,12,15,16]. In this model, the incoming projectile is represented by a plane wave and the active electron-target core bound state resulting from a Garvey potential, while the final three-body state is represented by the product of three distorted waves. In this prior version, the perturbation is given by the unsolved part of the initial Hamiltonian, i.e., the projectile-active electron interaction and the nuclear-nuclear interaction. Coulomb potentials are used to represent the interaction between the emitted electron and the projectile as well as the nuclear-nuclear interaction. In the latter, the target nuclear core charge is set equal to 1 since we restrict ourselves to high impact parameter collisions. Meanwhile, for the emitted electron-target interaction, three approximations are used and compared: model A, the effective charge derived from the formula for hydrogenic targets ($Z_{eff}=\sqrt{-2n^2\varepsilon}$) where n is the principal quantum number of the initial bound state; model B, the effective charge $Z_{eff}=1$ which represents the maximum possible screening of the nuclear charge by the passive electron; model C, the parametrization provided by Garvey *et al.* [19]. Model A has been extensively used providing qualitative agreement with the available experimental data for doubly differential cross sections as a function of the angle and energy of the emitted electron [20]. Treatments similar to model C, on the other hand, based on the numerical solution of the radial equation using a model potential, led to quantitative agreement with the available data [21,22]. Concerning the FDCS, both strategies have been used for He target but model C should be expected to lead to a more accurate description of the single ionization process as the number of passive electrons in the target increases.

The present FDCS is given by $d^5\sigma/d\mathbf{k}d\mathbf{Q}_\perp$, where $\mathbf{k}$ and $\mathbf{Q}_\perp$ indicate, respectively, the emitted electron momentum and the perpendicular component of the momentum transferred by the projectile.

In Fig. 1 we show the FDCS obtained with the present CDW calculation for electron emission from He impacted by protons in the scattering plane. The momentum transfer is $Q=0.4$ a.u. and the emitted electron energy $E_e=10$ eV. The effective target charge used with model A is $Z_{eff}=1.35$ which corresponds to an electron being emitted from the $1s$ state.

A large peak is present approximately in the direction of $\mathbf{Q}$ which can be attached to a binary collision between the projectile and the active target electron, while the other electron and the target nucleus remain passive. This structure is called the binary peak. A second peak appears as a consequence of the electron-residual target interaction and it is commonly referred to as the recoil peak. As was demonstrated by Gasaneo *et al.* [7] within the first Born approximation, this recoil peak results from the splitting of the soft peak. When a Coulomb potential is assumed for the interaction between the active electron and the residual target, the ionization transition matrix contains a Coulomb factor that

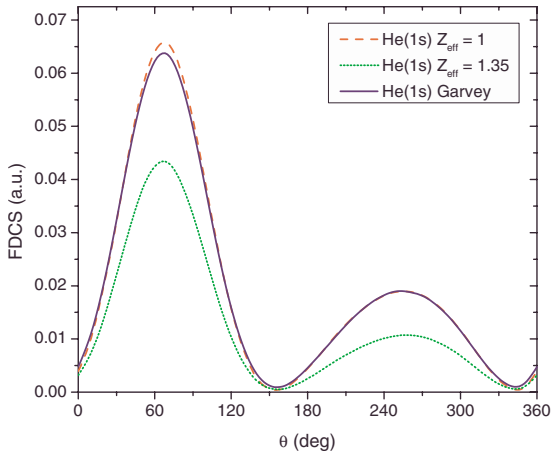

FIG. 1. (Color online) FDCS in the collision plane as a function of the electron emission angle (θ) for 2 MeV/amu H^++He, $Q=0.4$ a.u., and $E_e=10$ eV. Theories: model A (···), model B (- - -), and model C (—).

diverges for $k\to 0$ and gives the soft electron emission peak. A form factor proportional to the bound-continuum oscillator strength modulates this divergence and splits that peak in two [7].

This effect can be viewed in the contour plot graphics shown in Figs. 4–6 as a trench that cuts the low energy profile of the soft peak and crosses the momentum space origin. For a fixed electron energy these features can be observed in Fig. 1.

Although different choices for the model potential do not affect the general features of the FDCS, i.e., the binary and recoil structures, the explicit shape of the peaks are sensitive to the choice. It can be seen that models B and C lead to similar angular distributions which are about a factor 1.5 higher than the predictions provided by model A.

In Fig. 2 we consider the Li target keeping the same momentum transfer, emitted electron energy, and projectile impact energy. The effective charge for model A is $Z_{eff}=1.25$ which corresponds to an electron being emitted from the $2s$ state. In this case, side shoulders appear around the binary

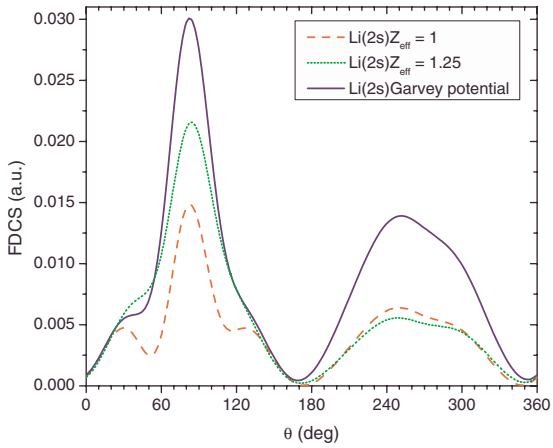

FIG. 2. (Color online) Same as in Fig. 1 for 2 MeV/amu H^++Li.

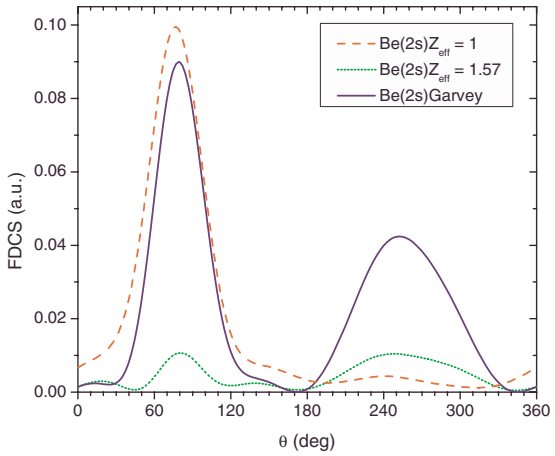

FIG. 3. (Color online) Same as in Fig. 1 for 2 MeV/amu H^++Be.

peak and, in general, the three models lead to different angular distributions. While models A and B provide a similar description of the recoil peak, there is no coincidence among the models on the binary peak region. On the other hand, all the models evidence a binary peak with structure on the sides which can be attributed to the 2*s* nature of the initially bound electron.

In Fig. 3 we consider the Be target under the same conditions shown in Figs. 1 and 2. The effective charge for model A is $Z_{eff}=1.57$ which corresponds to an electron being emitted from the 2*s* state. In this case models B and C lead to a similar description of the binary peak, but the recoil peak predicted by model C is almost a factor 10 higher. This is a consequence of the Garvey potential which allows the electron to see a nuclear charge $Z=1$ at large distances and the full target nucleus charge at short distances. It is well known that this sort of potential leads in scattering problems to the "rainbow" effect studied in the classical context by Ford and Wheeler [23], that evidences through oscillations in the scattering amplitude as a function of the emission angle and an increase in the intensity of the 180° emission. A good description of such oscillations was performed by Schultz and Olson [24,25]. The final continuum state for the electron and residual target contains an increasing number of single virtual collisions between these particles, given by each term in the perturbative expansion. There is a relevant difference between the continuum state resulting from a Garvey potential and a Coulomb wave. The former allows for a different dynamics in each perturbative order, leading to a much higher recoil peak.

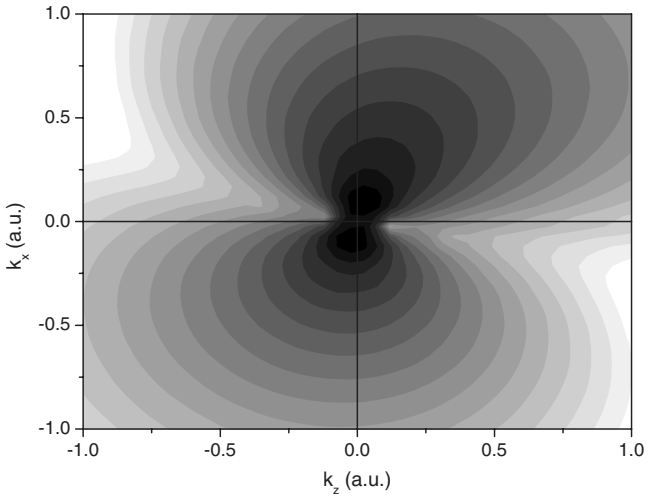

FIG. 4. FDCS (on a logarithmic scale) in the collision plane as a function of the transverse (k_x) and longitudinal (k_z) electron momenta for 2 MeV/amu H^++He.

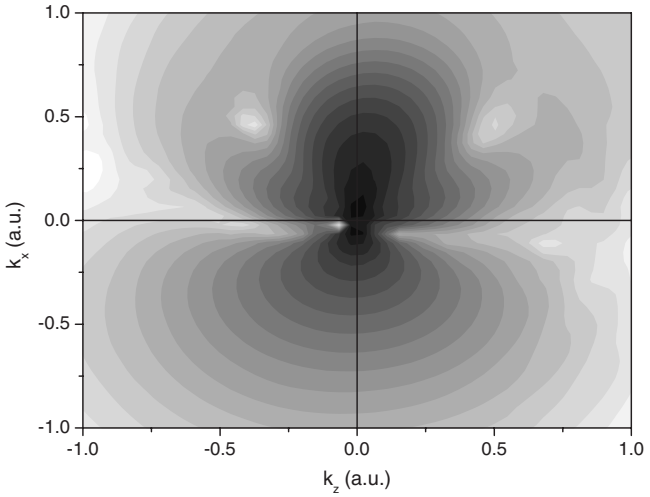

FIG. 5. Same as in Fig. 4 for 2 MeV/amu H^++Li.

In order to gain more insight into the structures that appeared on the sides of the binary peak in Figs. 2 and 3, we now show in Figs. 4–6 FDCS calculated with model C, represented in the momentum space of the emitted electron and we focus on the soft peak region. The angular distributions shown above can then be simply understood as the profile of a circular cut of the FDCS in momentum space. For He, a trench is clearly visible which separates the binary peak from the recoil peak at different energies. For Li and Be, we see

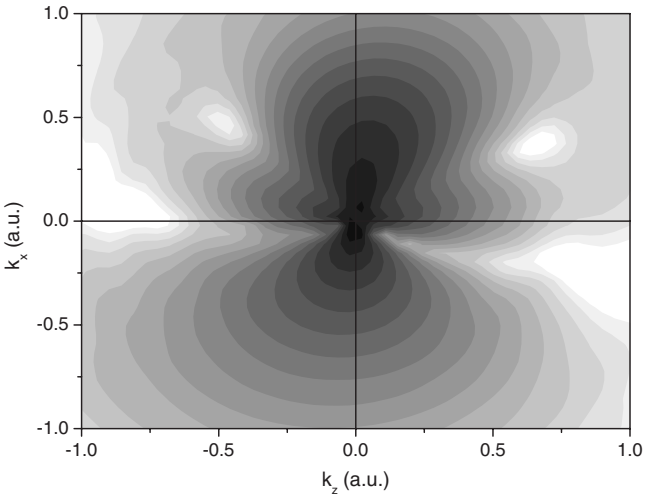

FIG. 6. Same as in Fig. 4 for 2 MeV/amu H^++Be.

that the binary peak has shoulders at different emission energies indicating that they are not due to the particular configuration chosen in Figs. 2 and 3 but evidence a more general trend instead. We have performed similar calculations by using the simple first Born approximation which completely neglects the postcollisional interaction and found the same features which we then attach to the initial state. Such structures are predicted by the three models here employed, although the shapes and intensities vary from one another.

To summarize, we have calculated FDCSs for proton impact on multielectronic targets and studied the main differences found with the well known results from previous studies on He atoms. For Li and Be, we have found shoulders on the sides of the binary peak which can be attributed to the 2*s* nature of the initially bound electron. This shows that FDCSs on multielectronic systems do not only lead to the familiar binary and recoil peaks present for the well documentated He target, but instead evidence more richness and complexity. Furthermore, for multielectronic targets, the use of a model potential like the Garvey representation for the emitted electron-target interaction should be more appropriate and it should be expected to provide a more accurate representation of the recoil peak compared to Coulomb treatments assuming effective charges.

The recent inclusion of a lithium MOT in a reaction microscope gives hope of soon to come data which would not only revitalize the field, but challenge theoreticians to provide an accurate description of the ion-Li collision system.

Work was supported by PGI F24/F038 (UNS), PICTR 03/437 of the ANPCyT, and PIP 5595 of the CONICET (Argentina).

[1] J. Ullrich, R. Moshammer, R. Dörner, O. Jagutzki, V. Mergel, H. Schmidt-Bocking, and L. Spielberger, J. Phys. B **30**, 2917 (1997).
[2] R. Dörner *et al.*, Phys. Rev. Lett. **72**, 3166 (1994); R. Moshammer, J. Ullrich, M. Unverzagt, W. Schmidt, P. Jardin, R. E. Olson, R. Dörner, V. Mergel, U. Buck, and H. Schmidt-Böcking, *ibid.* **73**, 3371 (1994).
[3] H. Erhardt, M. Schulz, T. Tekaat, and K. Willmann, Phys. Rev. Lett. **22**, 89 (1969).
[4] M. Schulz *et al.*, J. Phys. B **34**, L305 (2001); L. An, Kh. Khayyat, and M. Schulz, Phys. Rev. A **63**, 030703(R) (2001).
[5] D. Fischer, R. Moshammer, M. Schulz, A. Voitkiv, and J. Ullrich, J. Phys. B **36**, 3555 (2003); M. Schulz, A. Hasan, N. V. Maydanyuk, M. Foster, B. Tooke, and D. H. Madison, Phys. Rev. A **73**, 062704 (2006).
[6] J. Berakdar, J. S. Briggs, and H. Klar, J. Phys. B **26**, 285 (1993).
[7] G. Gasaneo, W. R. Cravero, M. D. Sanchez, and C. R. Garibotti, Phys. Rev. A **54**, 439 (1996).
[8] M. D. Sánchez, W. R. Cravero, and C. R. Garibotti, Phys. Rev. A **61**, 062709 (2000).
[9] M. D. Sánchez, W. R. Cravero, and C. R. Garibotti, Nucl. Instrum. Methods Phys. Res. B **142**, 281 (1998).
[10] C. J. Wood, C. R. Feeler, and R. E. Olson, Phys. Rev. A **56**, 3701 (1997).
[11] D. H. Madison, M. Schulz, S. Jones, M. Foster, R. Moshammer, and J. Ullrich, J. Phys. B **35**, 3297 (2002).
[12] J. Fiol and Olson, J. Phys. B **37**, 3947 (2004).
[13] R. E. Olson and J. Fiol, J. Phys. B **36**, L365 (2003).
[14] R. T. Pedlow, S. F. C. O'Rourke, and D. S. F. Crothers, Phys. Rev. A **72**, 062719 (2005).
[15] S. Otranto, R. E. Olson, and J. Fiol, J. Phys. B **39**, L175 (2006).
[16] J. Fiol, S. Otranto, and R. E. Olson, J. Phys. B **39**, L285 (2006).
[17] M. McCartney and D. S. F. Crothers, J. Phys. B **26**, 4561 (1993).
[18] J. Steinmann, invited talk at XX ISIAC 2007, Agios Nikolaos, Crete, Greece.
[19] R. H. Garvey, C. H. Jackman, and A. E. S. Green, Phys. Rev. A **12**, 1144 (1975).
[20] P. D. Fainstein, V. H. Ponce, and R. D. Rivarola, J. Phys. B **24**, 3091 (1991).
[21] L. Gulyas, P. D. Fainstein, and A. Salin, J. Phys. B **28**, 245 (1995).
[22] P. D. Fainstein and L. Gulyas, J. Phys. B **38**, 317 (2005).
[23] K. W. Ford and J. A. Wheeler, Ann. Phys. (N.Y.) **7**, 259 (1959).
[24] D. R. Schultz and R. E. Olson, J. Phys. B **24**, 3409 (1991).
[25] C. O. Reinhold, D. R. Schultz, R. E. Olson, C. Kelbch, R. Koch, and H. Schmidt-Böcking, Phys. Rev. Lett. **66**, 1842 (1991).